



# **Integrated Control of Floating Offshore Wind Farms with Reconfigurable Layouts**

Yue Niu<sup>1</sup> and Ryozo Nagamune<sup>1</sup>

<sup>1</sup>Department of Mechanical Engineering, University of British Columbia, 6250 Applied Science Lane, Vancouver, BC V6T1Z4, Canada

Correspondence: Yue Niu (niuyueubc@gmail.com)

#### Abstract.

This study proposes an integrated control method for floating offshore wind farms (FOWFs) that seeks to maximize farm-level power output or regulate it to a prescribed reference while mitigating wake-induced losses. To achieve these objectives, the method integrates existing control strategies: turbine repositioning, wake steering, power derating, and dynamic wake mixing, within a unified framework that adaptively selects the most effective combination based on wind conditions and control goals. This integration is motivated by the fact that individual strategies may be effective only under specific conditions or broadly effective but not always optimal, whereas their coordinated use can deliver robust performance improvements across a broad range of operating scenarios. The framework targets FOWFs with reconfigurable layouts, where turbines are mounted on floating platforms anchored to the seabed with sufficiently long and slack mooring lines, allowing them to shift within a certain range and thereby enabling controlled positional adjustments. Numerical simulations using the flow redirection and induction in steady state (FLORIS) engineering wake model show that the integrated method consistently outperforms any individual strategy. These findings highlight the potential of integrated control to enhance the efficiency, flexibility, and adaptability of FOWFs, offering a promising pathway to overcome the limitations and improve the performance of standalone control methods.

# 1 Introduction

The global shift toward sustainable energy demands a rapid expansion of offshore wind power, which offers immense potential for large-scale, clean electricity generation. By mounting turbines on buoyant platforms anchored to the seabed, floating offshore wind farms (FOWFs) extend offshore wind development into deepwater regions where fixed-bottom foundations are not feasible (Musial et al., 2022). This extension opens new geographical markets, allowing deployment in areas far from shore where winds are stronger and more consistent. Realizing this potential, however, requires addressing aerodynamic challenges that emerge when turbines are clustered into farms. As in onshore or fixed-bottom offshore wind farms, FOWFs are strongly affected by wake interactions. Each turbine extracts kinetic energy from the incoming wind, producing a downstream wake characterized by reduced wind speed and increased turbulence. When these wakes interact with downstream turbines, they reduce energy capture and accelerate fatigue loading. Such wake-induced effects can reduce total farm output by up to 20%, reducing project revenue and complicating reliable grid integration (Barthelmie et al., 2009). Mitigating wake losses is

Preprint. Discussion started: 19 November 2025

© Author(s) 2025. CC BY 4.0 License.





therefore critical to improving wind farm efficiency, ensuring stable power delivery, and meeting the ambitious offshore wind deployment targets set by many nations (Musial et al., 2022).

Wind farm control has been an active area of research for decades, aimed at mitigating wake effects and improving farm-wide performance (Boersma et al., 2017; Doekemeijer et al., 2019; Kheirabadi and Nagamune, 2019; Andersson et al., 2021; Dong et al., 2022). Among the various strategies, turbine repositioning through passive force generation (Niu et al., 2024; Han et al., 2017; Kheirabadi and Nagamune, 2020, 2021a, b; Gao et al., 2022; Niu et al., 2023; Jard and Snaiki, 2023; Kilinc, 2022; Mahfouz and Cheng, 2023) has emerged as a particularly promising approach. In this method, floating turbines are dynamically displaced to reduce wake overlap without the need for dedicated propulsion systems or additional mechanical actuators. Specifically, the displacement is achieved by exploiting aerodynamic forces on the rotor plane, for example, through intentional yaw misalignment, to generate thrust forces in the desired direction of motion. When combined with sufficiently long and slack mooring lines, these forces induce platform drift, enabling turbines to relocate to positions more favorable for both energy production and fatigue load reduction. Compared with propulsion-based repositioning methods, this passive strategy requires significantly less additional energy input and relies solely on actuators already available in modern utility-scale wind turbines, making it an attractive option for future deployment.

Despite its potential, this repositioning method has an inherent limitation: the extent of achievable crosswind displacement is strongly influenced by the relative angle between the incoming wind direction and the orientation of the mooring lines. When the wind direction is closely aligned with a mooring line, within about  $\pm 20$  degrees, the platform can drift laterally with relatively little resistance, enabling substantial repositioning and corresponding performance improvements (Kheirabadi and Nagamune, 2020). However, as the wind-mooring angle increases, the restoring stiffness of the mooring system rises sharply, restricting the platform's ability to move sideways. In such cases, the scope for crosswind repositioning diminishes, and the effectiveness of repositioning as a standalone strategy also becomes limited. One solution to overcome this limitation is to optimize farm layout prior to installation by carefully determining mooring line orientations across turbines so that at least a subset of turbines maintains sufficient mobility under any wind condition, as studied in (Froese et al., 2022). In contrast, the present study focuses on how to overcome this limitation assuming the farm layout is already fixed after installation.

To overcome this limitation, turbine repositioning can be complemented by other established wind farm control strategies, namely wake steering (Burton et al., 2011; Fleming et al., 2015), power derating (Steinbuch et al., 1988; Johnson and Thomas, 2009), and dynamic wake mixing (Goit and Meyers, 2015; van den Berg et al., 2024). These methods mitigate wake interaction through mechanisms that do not rely on large platform displacements and therefore remain effective when repositioning mobility is constrained. Specifically, wake steering redirects wakes away from downstream turbines by intentionally yawing upstream turbines, thereby reducing energy losses when repositioning cannot achieve sufficient lateral offset. Power derating lowers the thrust of selected upstream turbines, weakening their wakes and alleviating downstream loading. Dynamic wake mixing increases turbulent diffusion within the wake, thereby accelerating flow recovery and improving downstream inflow conditions. Importantly, these methods are inherently cooperative rather than competitive: repositioning is most effective when mobility is high, while wake steering, power derating, and dynamic wake mixing provide valuable alternatives when repositioning is limited. Combining these approaches therefore enables performance improvements across a wide range of wind and

Preprint. Discussion started: 19 November 2025

© Author(s) 2025. CC BY 4.0 License.





mooring conditions. This complementary relationship motivates the development of an integrated wind farm control framework that dynamically selects and coordinates these strategies according to wind conditions, platform mobility, and control objectives.

In this study, we propose an integrated wind farm controller for FOWFs with reconfigurable layouts that unifies turbine repositioning, wake steering, power derating, and dynamic wake mixing within a single optimization framework. The controller formulates wind farm control as an optimal control problem, solved using available measurements of wind speed and wind direction together with a prescribed farm-level power reference from the grid. The framework is designed to operate in two distinct modes, reflecting the main requirements of wind farm operation. In power maximization mode, the objective is to maximize total farm output, which is critical when the grid demands as much renewable power as possible. In power regulation mode, the objective is to track a prescribed power setpoint while simultaneously mitigating wake interactions, which is essential for grid stability. To achieve these objectives, the controller computes coordinated commands including yaw angles, power setpoints, and wake mixing intensities for each turbine and dispatches them to the corresponding turbine-level controllers for execution. The proposed approach is evaluated using the flow redirection and induction in steady state (FLORIS) engineering wake model (National Renewable Energy Laboratory), augmented with a steady-state turbine position solver. Simulation results across diverse wind conditions demonstrate that the integrated controller consistently outperforms any single control strategy. These results underscore the potential of integrated control to enhance farm performance, reduce operational costs, and strengthen the economic viability of large-scale deployment of reconfigurable FOWFs.

The remainder of the paper is organized as follows. Section 2 formulates the control problem for FOWFs with reconfigurable layouts. To address this problem, Sect. 3 presents the design of the integrated FOWF controller. Section 4 then evaluates the proposed controller through numerical simulations and provides a detailed analysis of its performance. Finally, Sect. 5 summarizes the main findings and outlines directions for future research.

## 2 Control Problem Formulation for FOWFs with Reconfigurable Layouts

This section formulates the control problem for FOWFs with reconfigurable layouts (Sect. 2.1). Specifically, we seek to design a wind farm controller that computes coordinated control inputs for the individual turbine controllers based on available information (Sect. 2.2), in order to achieve desired control objectives (Sect. 2.3). An illustrative example of this setup is shown in Fig. 1, which depicts an example FOWF equipped with a central wind farm controller. This schematic will serve as a reference throughout the formulation in this section.

## 2.1 FOWFs with Reconfigurable Layouts

Consider first the case of an FOWF without centralized coordination. Suppose N turbines are initially aligned in a row, as shown in the blue box of Fig. 1. The inflow is assumed steady and unidirectional, approaching from the left and first interacting with turbine 1. Because each turbine is mounted on a floating platform, its absolute position is not fixed; instead, the wind pushes the platform to a steady-state equilibrium where aerodynamic thrust is balanced by restoring forces from the mooring



100

105



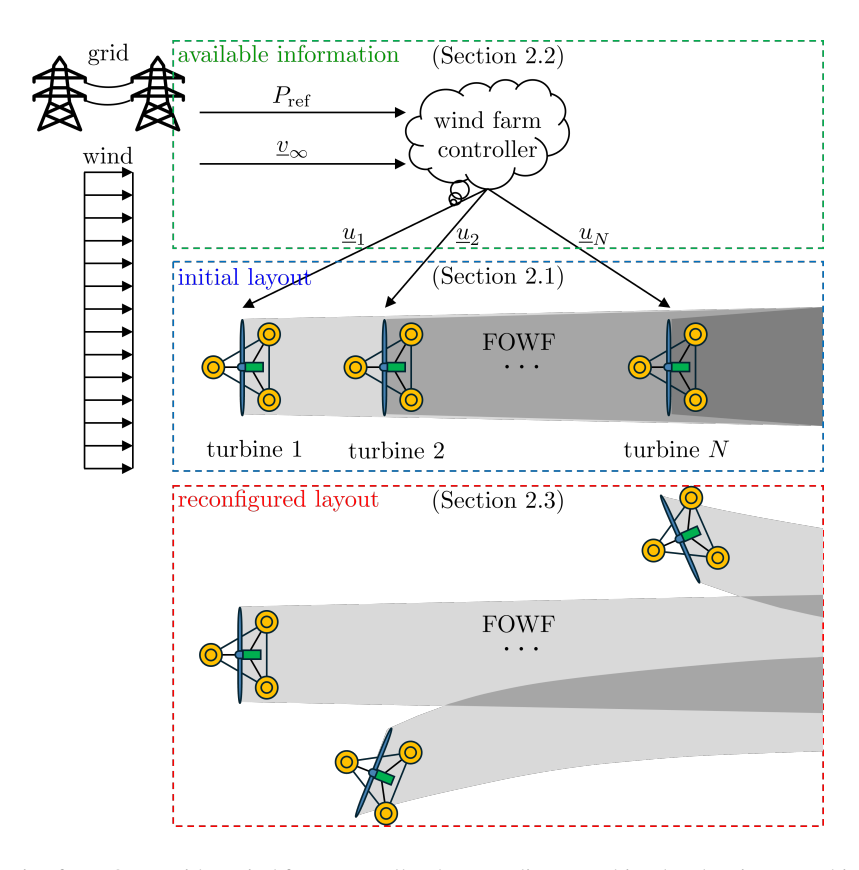


Figure 1. Top-view schematic of an FOWF with a wind farm controller that coordinates turbine-level actions to achieve farm-wide objectives.

lines. At this equilibrium, turbine 1 extracts energy from the flow at its rotor plane but also generates a wake of reduced wind speed, shown as a shaded gray region, which propagates downstream and interacts with turbine 2. This wake affects both the steady-state position and the power output of turbine 2. Turbine 2, in turn, produces its own wake (darker shade), further influencing subsequent turbines. This process continues across the farm, leading to cumulative wake interactions that reduce total energy production and impose unsteady loads on downstream rotors.

The inherent mobility of floating offshore wind turbines provides an opportunity to alleviate these challenges. As shown in Fig. 2, each turbine is mounted on a buoyant platform anchored to the seabed by mooring lines, which, if sufficiently long and slack, allow the platform to shift within a certain region. Referring to Fig. 3, controlled repositioning can be achieved by intentionally yawing the rotor away from the incoming wind, generating a lateral aerodynamic thrust that displaces the turbine to a new steady-state position. This mobility enables wind farm layouts to adapt dynamically to changing wind conditions, turbine health, and power requirements.

To fully exploit this capability and prevent the farm from operating at reduced efficiency under cumulative wake interactions, a supervisory wind farm controller is required. Such a controller can compute coordinated inputs for all turbines using the available farm-level information, thereby mitigating wake losses and improving overall performance.







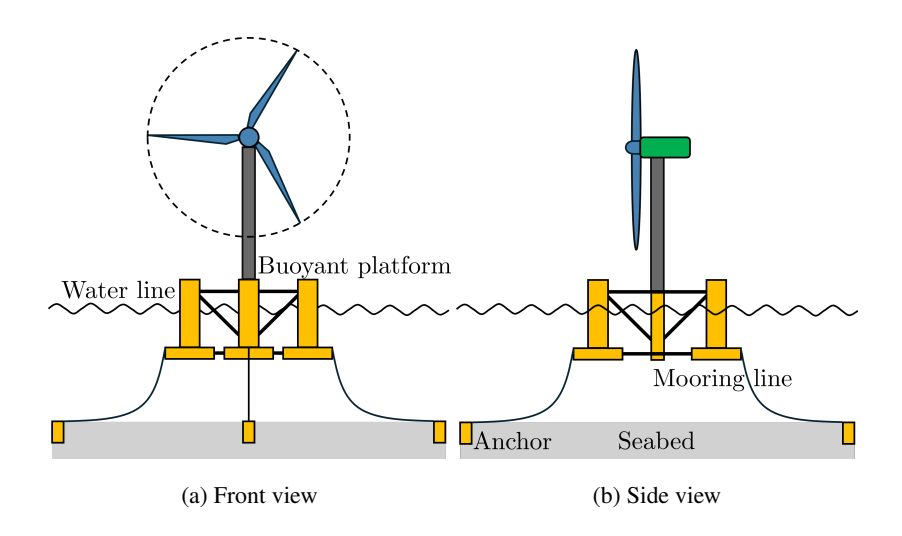


Figure 2. A floating offshore wind turbine mounted on a buoyant platform.

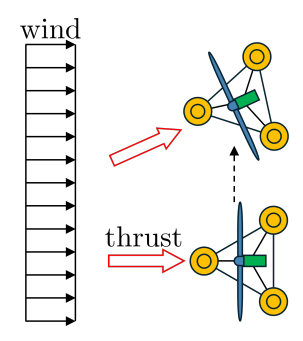


Figure 3. Turbine repositioning mechanism using yaw-induced aerodynamic forces.

## 2.2 Available Information and Control Inputs

The supervisory wind farm controller, shown in the green box of Fig. 1, is responsible for coordinating the operation of all turbines within the farm. It is assumed to have access to two key pieces of information: the farm-level power reference  $P_{\rm ref}$  (MW) provided by the grid, and the free-stream wind velocity  $\underline{v}_{\infty}$  (m/s) at hub height, defined as

110 
$$\underline{v}_{\infty} := \begin{bmatrix} v_{\infty,x} & v_{\infty,y} \end{bmatrix}^T$$
. (1)

Based on this information, the controller computes coordinated control inputs  $\underline{u}_i$  for all N turbines, where  $\underline{u}_i$  denotes the control input vector for turbine i with  $i=1,\ldots,N$ . The specific components of  $\underline{u}_i$  are introduced later in Sect. 3. At this stage, it suffices to note that  $\underline{u}_i$  represents the control actions commanded by the wind farm controller, specifying how each turbine should operate or be repositioned. Once computed, these inputs are dispatched to the individual turbine controllers (Fig. 1),

Preprint. Discussion started: 19 November 2025

© Author(s) 2025. CC BY 4.0 License.



120

135

140



which then execute the prescribed actions at the local level. Finally, the controller requires a specification of the farm-level objectives before determining the coordinated inputs.

## 2.3 Control Objectives for Wind Farm Controller

Through the available control inputs  $\underline{u}_i$ , the wind farm controller can pursue objectives that balance energy production with load mitigation. In this work, the control problem is formulated around two primary objectives:

- **Power maximization**: maximize the total electrical output of the wind farm.
- Power regulation: adjust farm power to track a prescribed reference  $P_{ref}$ . In this mode, wake mitigation is treated as an additional objective.

Power maximization is central to commercial wind farm operation, as maximizing energy capture directly improves economic returns and reduces the cost of electricity. By contrast, power regulation is particularly relevant for grid integration, where wind farms may be required to provide power setpoints consistent with system-level scheduling or ancillary service needs. Notably, power maximization can be regarded as a special case of power regulation by setting  $P_{\text{ref}}$  to the rated farm output. When operating in regulation mode, the controller additionally seeks to mitigate wake effects, thereby improving downstream flow conditions and reducing fatigue loading on downstream turbines.

The resulting problem is therefore to design a wind farm controller (Fig. 1) that, based on the available measurements  $P_{\text{ref}}$  and  $\underline{v}_{\infty}$ , computes optimal control inputs  $\underline{u}_i$ . These inputs are dispatched to individual turbine controllers to achieve one of the power objectives, while also mitigating wake effects. For example, as shown in the red box of Fig. 1, the coordinated control inputs instruct turbine 1 to maintain its position, while directing turbines 2 through N to displace in opposite crosswind directions to reduce wake overlaps. Through this cooperative adjustment, the turbines collectively reshape the flow field, mitigate wake interactions, and redistribute power generation across the farm. The result is a reconfigured wind farm layout in which all turbines act in harmony at new steady states. The detailed controller design is presented in the following section.

## 3 Integrated Wind Farm Controller Design

To realize the control objectives outlined in Sect. 2.3, we develop an integrated wind farm controller that unifies existing control strategies within a single optimization-based framework. The remainder of this section is organized as follows. Section 3.1 reviews the individual strategies that serve as building blocks of the integrated approach, while Sect. 3.2 presents the detailed design of the integrated controller.

## 3.1 Integrated Control Approach

A central challenge in wind farm operation is the presence of wake effects. As illustrated in Fig. 4a, an upstream turbine extracts energy from the incoming wind, creating a downstream region of reduced velocity and elevated turbulence. A downstream turbine operating within this wake not only produces less power but is also subjected to stronger unsteady loads, accelerating





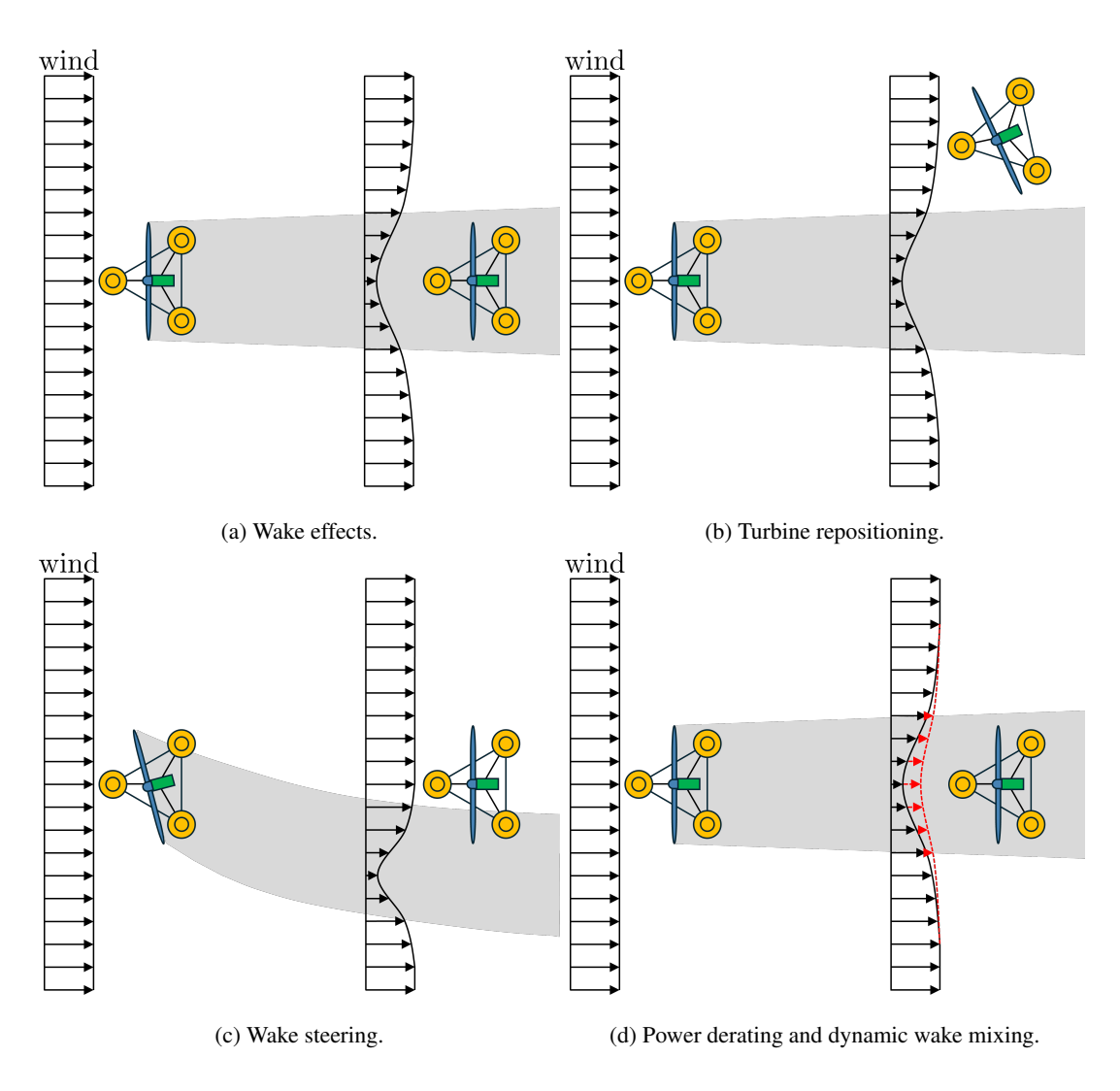


Figure 4. Illustration of wake effects and wind farm control strategies.





fatigue damage. At the farm scale, such interactions accumulate across multiple rows of turbines, significantly lowering overall energy yield while increasing maintenance costs.

These wake-induced losses motivate the development of advanced control strategies that actively manipulate the available inputs to mitigate interactions. For each turbine i, the control input vector introduced in Sect. 2.2 is defined as

$$\underline{u}_i := \begin{bmatrix} \theta_i & P_{\text{set},i} & \beta_{\text{amp},i} \end{bmatrix}^T, \tag{2}$$

where  $\theta_i$  (deg) is the net yaw angle,  $P_{\text{set},i}$  (MW) the power setpoint, and  $\beta_{\text{amp},i}$  (deg) the wake mixing intensity of turbine i, i = 1, ..., N. The remainder of this subsection reviews existing strategies and the ways in which they manipulate these control inputs.

#### 3.1.1 Turbine Repositioning and Its Limitation

Turbine repositioning sustains a net yaw angle  $\theta$  misalignment to generate lateral thrust forces, displacing the floating platform to a new equilibrium (Fig. 4b). The net yaw angle  $\theta$  quantifies the misalignment between the rotor plane and the incoming wind direction. It is defined as the sum of the nacelle yaw angle  $\gamma$  (deg) and the platform yaw angle  $\theta_z$  (deg), minus the inflow direction  $\angle \underline{v}_{\infty}$  (Fig. 5):

$$\theta = \gamma + \theta_z - \angle \underline{v}_{\infty}. \tag{3}$$

This positional change reduces overlap between the upstream wake and the downstream rotor, thereby enhancing energy capture and mitigating wake losses.

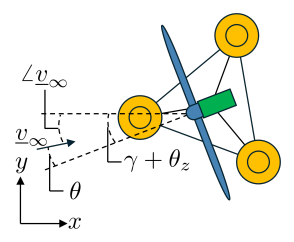


**Figure 5.** Definition of net yaw angle  $\theta$ .

165

Despite its potential, turbine repositioning with passive thrust generation faces an inherent limitation: the extent of achievable crosswind displacement depends strongly on the relative angle between the incoming wind direction and the orientation of the mooring lines. As illustrated in Fig. 6a, the turbine is initially at its neutral position in the absence of wind. When the wind direction is closely aligned with a mooring line, as shown in Fig. 6b (wind from the left, with a relative angle of 0 degrees), and assuming a net yaw angle of  $\theta = 0$ , the turbine is first displaced downwind until the aerodynamic force is balanced by the mooring line forces. At this new equilibrium, the two mooring lines highlighted in the figure become slack. Consequently, the platform can drift laterally with little resistance, enabling substantial repositioning and corresponding performance improvements. By contrast, as the wind-mooring angle increases, the platform mobility is greatly reduced. An example is shown in

Preprint. Discussion started: 19 November 2025

© Author(s) 2025. CC BY 4.0 License.



185

190

195



Fig. 6c, where the wind comes from the right, representing the worst case with a relative angle of 60 degrees. As before, the turbine shifts downwind until a new equilibrium is reached. However, in this case the same two mooring lines are placed in tension. The resulting restoring forces of the mooring lines rise sharply, severely restricting lateral motion and reducing the effectiveness of repositioning.

Quantitatively, numerical studies (Kheirabadi and Nagamune, 2020) have shown that increasing the relative angle from 0 to 20 degrees reduces achievable crosswind displacement from 139.6 m (1.1 D, where D denotes rotor diameter) to 97.7 m (0.8 D). A further increase to 40 degrees decreases mobility drastically to only 8.95 m (0.1 D), limiting the effectiveness of turbine repositioning. In such cases, wake losses can no longer be mitigated effectively. To overcome this limitation, repositioning can be combined with other strategies, including wake steering, power derating, and dynamic wake mixing.

## 3.1.2 Other Standalone and Integrated Control Methods

When platform mobility is limited, the same net yaw angle  $\theta$  can be used to deflect the wake laterally without displacing the platform (Fig. 4c). This deliberate misalignment steers the wake away from the downstream turbine, improving its inflow conditions. Although generally less effective than repositioning, wake steering remains applicable across a wider range of wind directions.

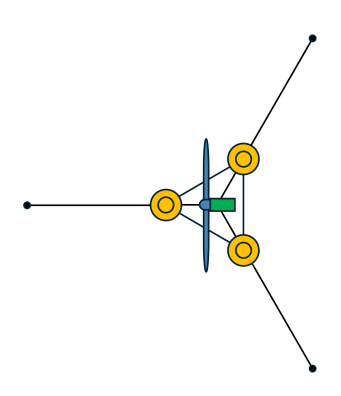
Power derating (Fig. 4d) reduces aerodynamic loading on selected turbines by constraining their power outputs to prescribed power setpoints  $P_{\text{set}}$ . By extracting less energy from the inflow, derated turbines generate wakes with smaller velocity deficits and reduced turbulence intensity, thereby improving flow conditions for downstream turbines and reducing fatigue-inducing structural loads across the farm.

Dynamic wake mixing (Fig. 4d) enhances turbulent diffusion to accelerate wake recovery. It is implemented through periodic variations in blade pitch angles, with the oscillation amplitude denoted by  $\beta_{amp}$ . These excitations promote faster entrainment of high-energy air into the wake, thereby improving the inflow conditions for downstream turbines.

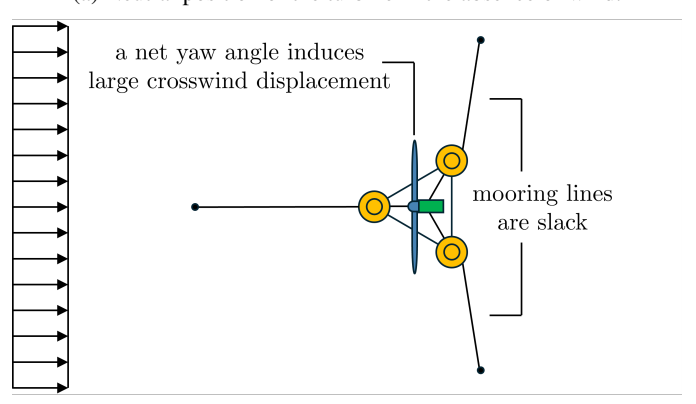
While each strategy provides distinct benefits, their combined application enables more flexible and effective farm-wide operation across diverse wind conditions. By integrating turbine repositioning, wake steering, power derating, and dynamic wake mixing within a unified optimization framework, the controller can adaptively select and coordinate strategies based on wind conditions and control objectives. This integrated approach enhances robustness by ensuring that farm-level performance does not hinge on the availability of a single control method. For example, when platform mobility is high, repositioning can be prioritized, whereas in constrained orientations, wake steering, power derating, and dynamic wake mixing can take over.



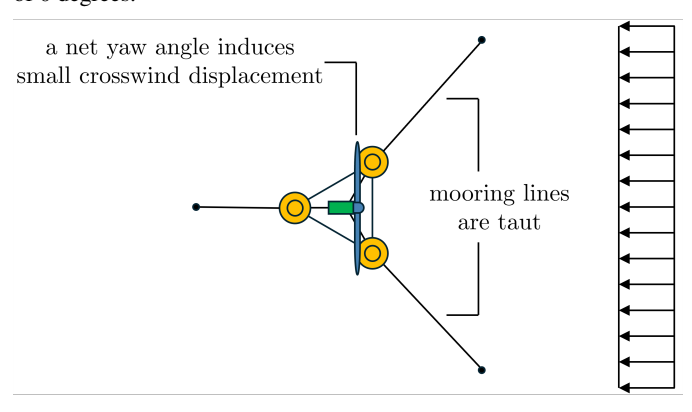




(a) Neutral position of the turbine in the absence of wind.



(b) Favorable wind direction: wind from the left, with a relative angle of 0 degrees.



(c) Unfavorable wind direction: wind from the right, with a relative angle of 60 degrees.

Figure 6. Illustration of the limitation of turbine repositioning.

10

Preprint. Discussion started: 19 November 2025

© Author(s) 2025. CC BY 4.0 License.



200

205



## 3.2 Integrated Controller Design

The integrated controller computes the optimal control inputs  $\underline{u}_i$  by solving a constrained optimization problem formulated as

$$\min_{u_i} J(\underline{u}_i) \tag{4a}$$

s.t. Wake model: 
$$[P_i, \underline{v}_i, C_{t,i}] = f_{\text{FLORIS}}(\underline{x}_i, \underline{v}_{\infty}, \underline{u}_i),$$
 (4b)

Equilibrium constraint: 
$$\underline{F}_{aero,i}(\underline{v}_i, C_{t,i}) + \underline{F}_{moor,i}(\underline{x}_i) = \underline{0},$$
 (4c)

Operational constraint: 
$$\underline{u}_{\min} \le \underline{u}_i \le \underline{u}_{\max}$$
. (4d)

Here,  $J(\cdot)$  denotes the cost function that encodes the control objectives (Sect. 3.2.1). The wake model  $f_{FLORIS}(\cdot)$  captures aerodynamic interactions among turbines and predicts steady-state power production (Sect. 3.2.2). The constraints include equilibrium conditions balancing aerodynamic and mooring forces, as well as operational limits on the inputs (Sect. 3.2.3). The resulting nonlinear, nonconvex problem is solved numerically using the methods described in Sect. 3.2.4.

### 3.2.1 Objective Function

The cost function  $J(\cdot)$  in (4a) is defined as

$$J(\underline{u}_i) = w_P (P_{\text{ref}} - \sum_{i=1}^N P_i)^2 + w_v \sum_{i=1}^N \|\underline{v}_{\infty} - \underline{v}_i\|^2,$$
(5)

where  $w_P$  and  $w_v$  are weighting coefficients. This objective function balances competing control objectives through weighted penalties. The first term enforces power-related objectives: for power maximization,  $P_{\text{ref}}$  is set to the farm's rated capacity, whereas for power regulation it corresponds to a prescribed farm-level target. Deviations of the actual output  $\sum_{i=1}^{N} P_i$  from this reference are penalized accordingly. The second term promotes wake mitigation by penalizing discrepancies between the free-stream wind velocity  $\underline{v}_{\infty}$  and the local velocity  $\underline{v}_i$  at the rotor of turbine i. Collectively, these terms enable the controller to satisfy power objectives while simultaneously reducing wake interactions.

## 215 **3.2.2 Wake Model**

The turbine power  $P_i$  in (4b) is estimated using FLORIS (National Renewable Energy Laboratory), an engineering wake model developed by the U.S. National Renewable Energy Laboratory. FLORIS is computationally efficient and well suited for control applications, providing steady-state predictions of farm performance under different operating conditions. The model captures the effects of yaw misalignment, induction, and wake interactions, using as inputs the turbine locations  $\underline{x}_i$ , free-stream wind conditions, and control inputs. This enables the controller to rapidly evaluate the impact of candidate control actions  $\underline{u}_i$  on overall farm power output.

https://doi.org/10.5194/wes-2025-240 Preprint. Discussion started: 19 November 2025

© Author(s) 2025. CC BY 4.0 License.



225

235

240



#### 3.2.3 Constraints

The optimization problem incorporates both equilibrium and operational constraints in (4c) and (4d). First, each turbine must satisfy static force equilibrium between the aerodynamic thrust and the restoring forces of the mooring system to maintain stable positioning. The aerodynamic thrust force on turbine i is given by

$$\underline{F}_{\text{aero},i} := \frac{1}{2} \rho A \|\underline{v}_i\| C_{t,i} \underline{v}_i, \tag{6}$$

where  $\rho$  (kg/m<sup>3</sup>) is the air density, A (m<sup>2</sup>) is the rotor swept area,  $\underline{v}_i$  (m/s) is the inflow velocity at the rotor plane, and  $C_{t,i}$  (-) is the thrust coefficient.

In addition, all control inputs are constrained by minimum and maximum bounds,  $\underline{u}_{\min}$  and  $\underline{u}_{\max}$ , which ensure  $\underline{u}_i$  remains within physically realizable and safe operating ranges. Together, the equilibrium and operational constraints preserve turbine stability while preventing infeasible or overly aggressive control actions.

#### 3.2.4 Solution Method and Implementation

The wake model and the force equilibrium in (4) are solved simultaneously using an iterative procedure. Given the free-stream wind velocity  $\underline{v}_{\infty}$  and the candidate control inputs  $\underline{u}_i$ , initial turbine positions  $\underline{x}_i$  are assumed and passed to FLORIS to compute the local velocity  $\underline{v}_i$  and thrust coefficient  $C_{t,i}$  for each turbine. From these values, the aerodynamic thrust  $\underline{F}_{\text{aero},i}$  and the corresponding mooring line force  $\underline{F}_{\text{moor},i}$  required for equilibrium are determined. A precomputed look-up table, generated from a quasi-static model (Jonkman, 2009), is then used to update the turbine positions  $\underline{x}_i$  corresponding to the calculated mooring forces. The updated positions are fed back into FLORIS to recompute  $\underline{v}_i$  and  $C_{t,i}$ , and this process repeats until the turbine positions converge. Once convergence is achieved, the turbine power and local velocities obtained from FLORIS are used to evaluate the cost function in (5).

Overall, the optimization problem formulated in (4) is nonlinear and nonconvex because of the complex wake interactions and spatial constraints. To solve it, we employ the non-dominated sorting genetic algorithm II (NSGA-II) (Deb et al., 2002), an evolutionary optimization method well suited for complex, nonconvex problems. The next section presents simulation results that demonstrate the performance of the proposed controller under a wide range of wind conditions.

## 245 4 Simulation Results

This section evaluates the performance of the wind farm controller through simulations conducted with the FLORIS engineering wake model. The simulations serve as a validation of the optimization framework developed in Sect. 3, demonstrating the controller's ability to maximize total power output and regulate farm-level power to a desired reference. In addition, they assess how effectively the controller mitigates wake effects. We first describe the simulation setup and test scenarios (Sect. 4.1), before presenting and discussing the comprehensive results (Sect. 4.2).



255



## 4.1 Simulation Setup and Scenarios

## 4.1.1 Simulation Setup

The case study considers an FOWF with a reconfigurable layout comprising 10 turbines. The farm layout is shown in Fig. 7, and the corresponding turbine neutral positions are listed in Table 1. Each turbine is modeled as the NREL 5MW offshore reference wind turbine (Jonkman et al., 2009) mounted on a semisubmersible platform (Robertson et al., 2014). Turbine, platform, and mooring system parameters follow the standard specifications in (Jonkman et al., 2009; Robertson et al., 2014), with one key modification: the mooring line length is extended to 970 m. This extension expands the feasible motion range of each turbine, enabling controlled repositioning and allowing the wind farm layout to adapt dynamically to changing wind conditions. The admissible control inputs in (4d) are defined as  $\underline{u}_{\min} = [-20, 4, 0]$  and  $\underline{u}_{\max} = [20, 5, 5]$ .

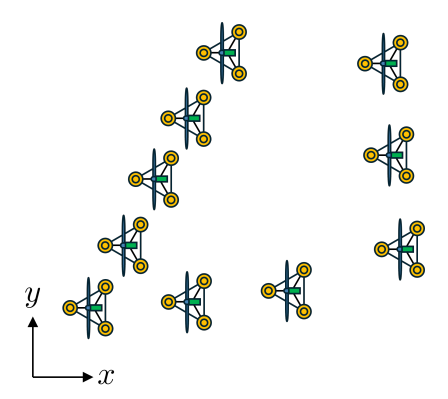


Figure 7. Example layout of the 10-turbine FOWF.

**Table 1.** Neutral positions of turbines in the case-study FOWF, normalized by rotor diameter  $D=126~\mathrm{m}$ .

Turbine	(x/D,y/D) (-)	Turbine	(x/D,y/D) (-)
1	(0,0)	6	(5.00,12.35)
2	(1.76,4.12)	7	(16.03, 3.82)
3	(5.00,0.44)	8	(6.76,16.47)
4	(3.24,8.24)	9	(15.44,10.00)
5	(10.15, 1.03)	10	(15.15,15.88)

### 260 4.1.2 Simulation Scenarios

Controller performance is evaluated under two representative scenarios:

- Power maximization: the controller seeks to maximize total farm output.





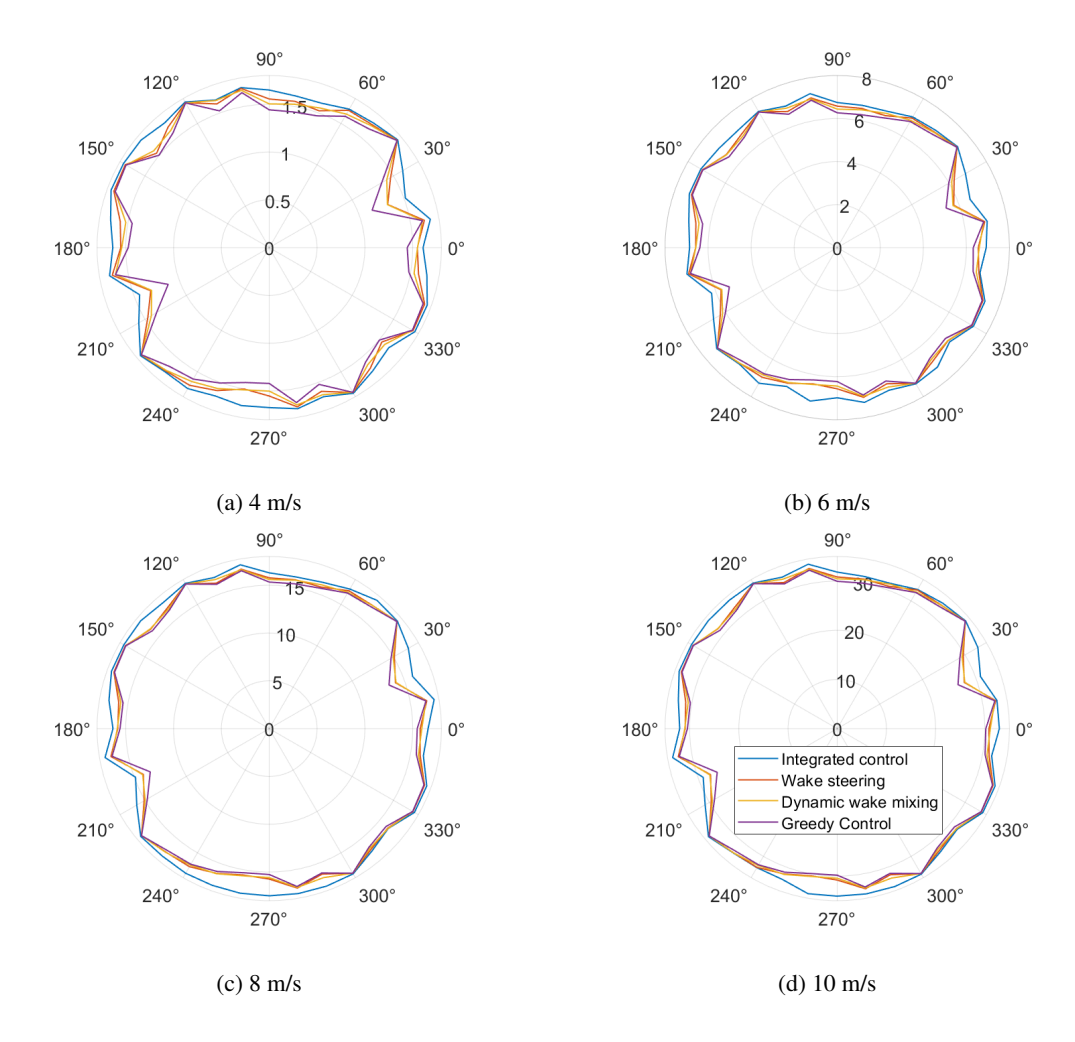


**Figure 8.** Maximum farm power across wind directions for integrated control, wake steering, dynamic wake mixing, and greedy control at inflow speeds of 4, 6, 8, and 10 m/s.

- Power regulation with wake penalties: the controller tracks a prescribed power reference  $P_{\text{ref}}$ , while also reducing wake overlap.
- For these scenarios, inflow conditions are modeled as steady winds with representative speeds selected between the cut-in limit of 3 m/s and the cut-out limit of 25 m/s, and directions spanning the full 0-360 degrees range. Ocean wave effects are neglected.





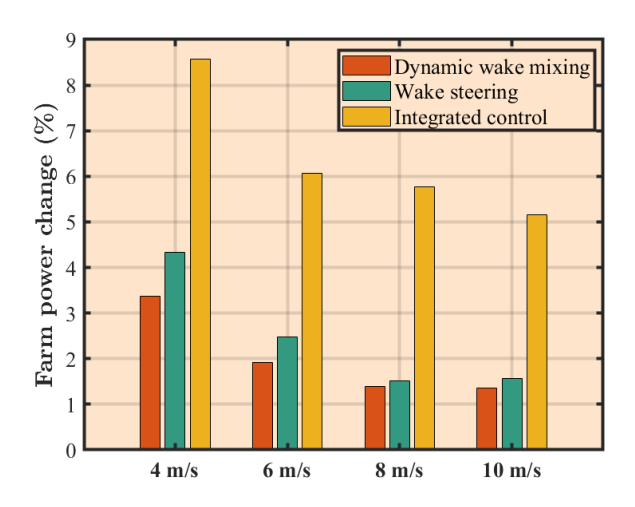


Figure 9. Average maximum farm power over all wind directions for inflow speeds between 4 and 10 m/s.

## 4.2 Results

275

280

# 4.2.1 Power Maximization

The proposed integrated controller, which combines turbine repositioning, wake steering, and dynamic wake mixing, is bench270 marked against the individual strategies of wake steering, dynamic wake mixing, and greedy control. Here, greedy control
refers to the baseline operation in which each turbine independently maximizes its own power production without coordination across the farm. Power derating is excluded from this comparison because FLORIS simulations consistently show that it
produces lower total output than greedy control across all wind speeds and inter-turbine spacings.

Fig. 8 shows the maximum achievable farm power across wind directions for inflow speeds of 4, 6, 8, and 10 m/s. Each plot compares the different strategies, with the numbers displayed inside each plot indicating the wind farm power in megawatts. For higher wind speeds, results are not presented because even turbines in wake regions encounter above-rated inflow, allowing greedy control alone to deliver rated farm power. Across all reported cases, the integrated controller consistently outperforms the individual strategies.

To summarize overall performance, Fig. 9 reports the average maximum farm power over all wind directions for inflow speeds between 4 and 10 m/s. The bar plots show the relative improvements of the integrated controller, wake steering, and dynamic wake mixing compared to greedy control. The integrated controller achieves the highest mean output at all wind speeds considered, outperforming individual strategies by up to 8.6%. These results demonstrate the clear benefit of coordinating multiple control mechanisms within a unified framework.

To further illustrate how the integrated approach leverages different strategies, two representative cases are shown in Figs. 10 and 11 for a wind speed of 10 m/s, with inflow coming from the west and southwest, respectively. Each figure includes three





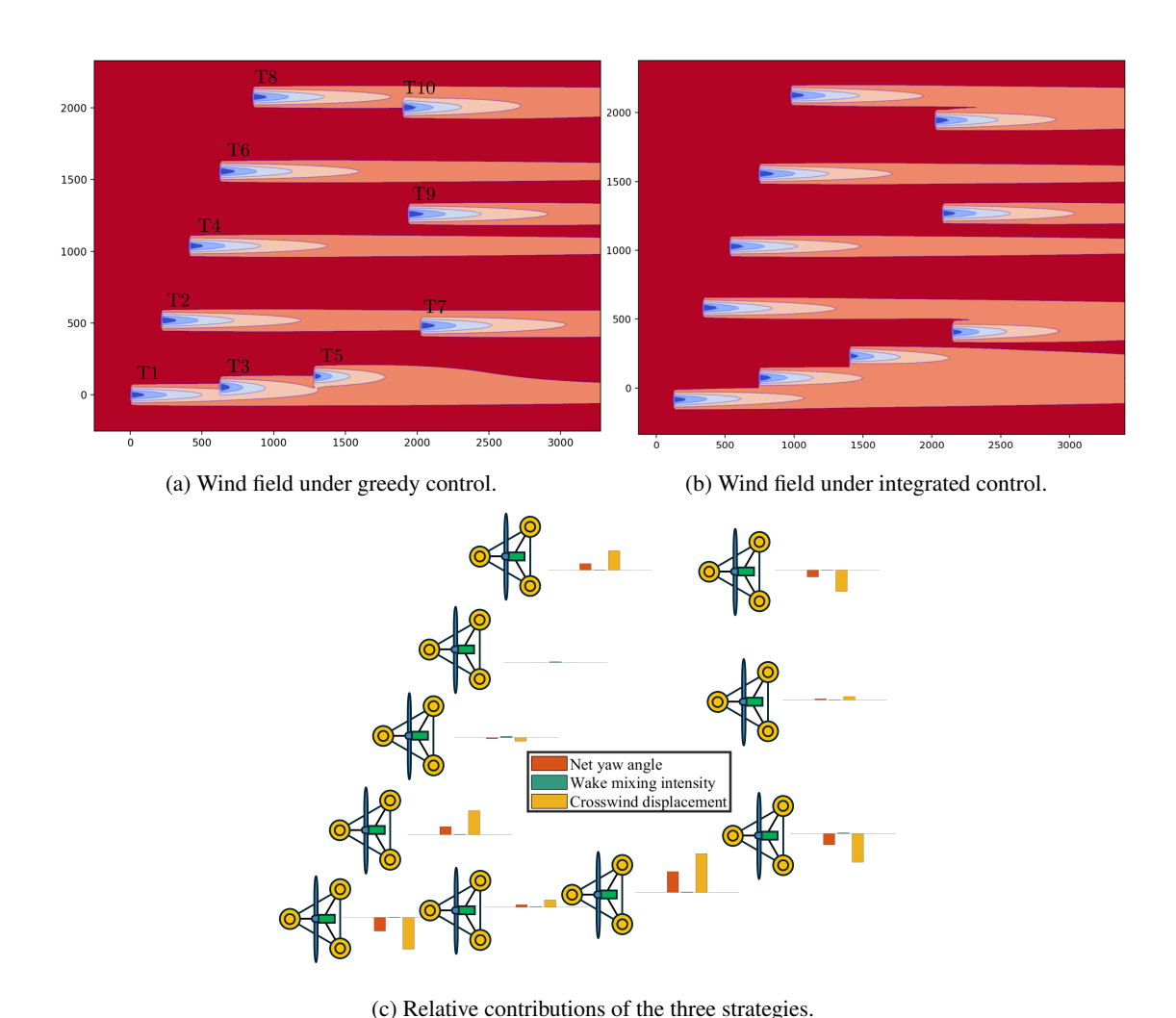


Figure 10. Control strategy contributions at a wind speed of 10 m/s with inflow from the west.

panels: (a) the wind field under greedy control, (b) the wind field under integrated control, and (c) a bar plot for each turbine showing the relative contribution of the three strategies. In the wind field plots, color represents wind speed, with red indicating free-stream wind speed and white/blue denoting wake regions. In the bar plots, the net yaw angle, wake mixing intensity, and crosswind displacement are normalized by their respective maximum values.

In Fig. 10, where the wind originates from the west, turbines have substantial crosswind mobility. Consequently, turbine repositioning is prioritized to mitigate wake effects and enhance overall farm power. For example, to reduce wake interactions among Turbines 1, 3 and 5, Turbine 1 applies a negative net yaw angle to shift downward, Turbine 3 remains almost at the same position, and Turbine 5 applies a positive net yaw angle to shift upward. As a result, all three turbines gain access to





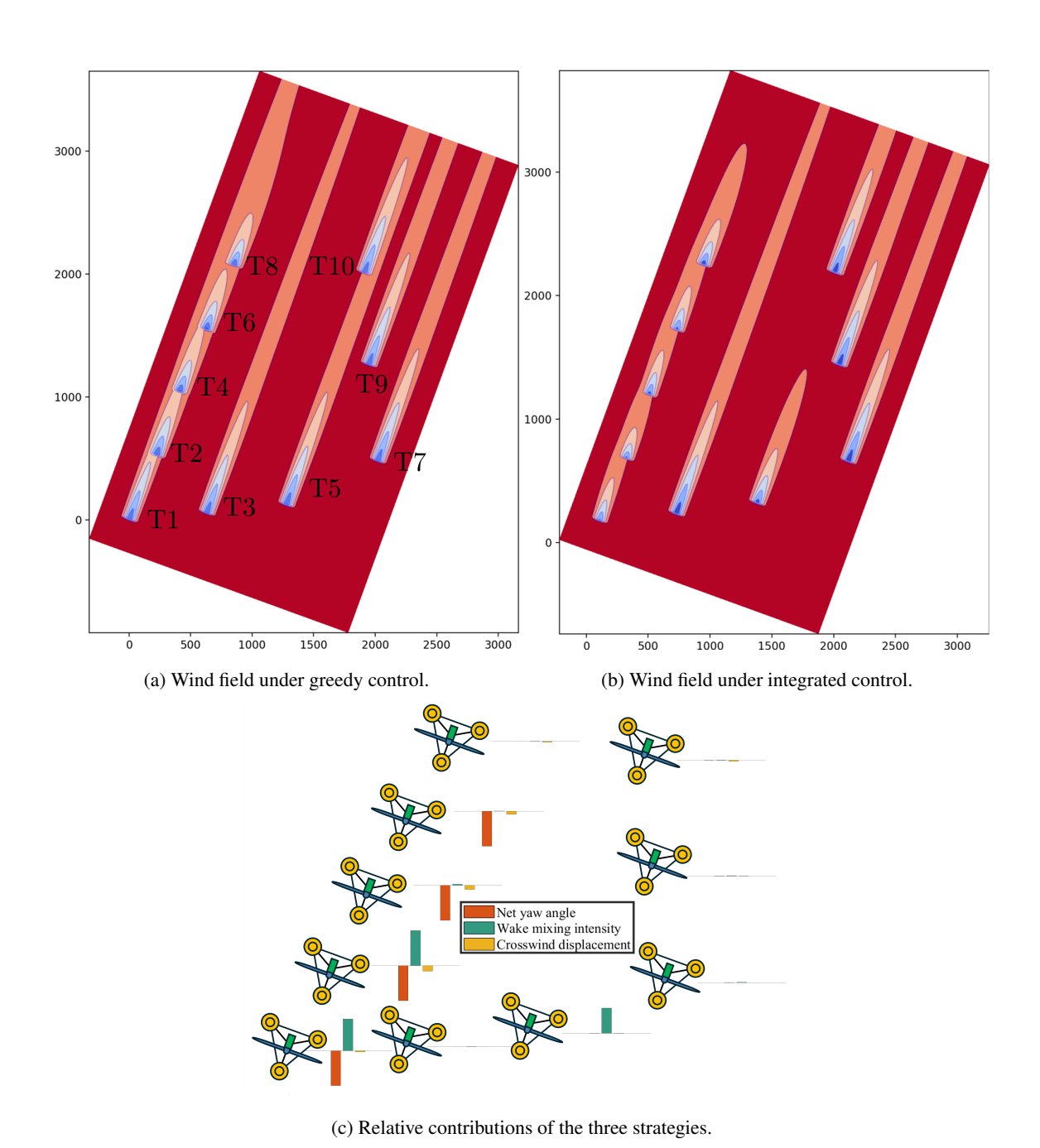


Figure 11. Control strategy contributions at a wind speed of 10 m/s with inflow from the southwest.

Preprint. Discussion started: 19 November 2025

© Author(s) 2025. CC BY 4.0 License.



295

300



free-stream wind and generate higher overall power. Similarly, wake interactions between Turbines 2 and 7, as well as between Turbines 8 and 10, are alleviated by repositioning the turbines in opposite crosswind directions.

By contrast, when the wind originates from the southwest (Fig. 11), crosswind mobility is limited, and wake steering together with dynamic wake mixing become the dominant strategies. To mitigate wake interactions among Turbines 1, 2, 4, 6, and 8, Turbines 1 and 2 rely on a combination of wake steering and dynamic wake mixing, while Turbines 4 and 6 employ wake steering alone. Turbine 8, being the most downstream turbine, makes no adjustment. In addition, Turbine 5 applies dynamic wake mixing to enhance the inflow to Turbine 10. The remaining Turbines 3, 7, and 9 are unaffected by wakes and therefore remain unchanged. Overall, these cases highlight how the integrated controller adaptively coordinates strategies to maximize performance under varying wind conditions.

## 4.2.2 Power Regulation with Wake Penalties

This case study investigates how the integrated controller achieves farm-level power regulation while accounting for wakeoverlap penalties, simultaneously employing turbine repositioning, wake steering, and power derating. The analysis is conducted for an inflow speed of 18 m/s, with the farm-level reference power set to  $P_{\text{ref}} = 45$  MW. Results are presented in
Figs. 12 and 13 for westerly and southwesterly inflow conditions, respectively. Each figure includes three panels similar to
those used for the power maximization case, except that the bar plots in panel (c) show normalized power setpoints in place of
wake mixing intensity.

For the westerly case (Fig. 12), all turbines apply some degree of power derating to satisfy the farm-level reference. At the same time, their high crosswind mobility enables repositioning to serve as the primary means of wake mitigation. Similar to Fig. 10, coordinated crosswind shifts between Turbines 1 and 5 relative to Turbine 3, between Turbines 2 and 7, and between Turbines 8 and 10 collectively reduce wake overlap across the farm.

By contrast, under southwesterly inflow (Fig. 13), limited crosswind mobility constrains repositioning, making wake steering the prevailing strategy. Turbines 1, 2, 4, and 6 actively redirect their wakes by alternating between positive and negative yaw angles to reduce wake overlap. In addition, Turbine 5 steers its wake away from Turbine 10 to improve its inflow. Overall, these results demonstrate that the integrated controller not only ensures reliable power tracking through power derating but also adaptively prioritizes between repositioning and wake steering, depending on inflow direction and available turbine mobility, to effectively mitigate wake effects.

### 320 5 Conclusions

325

This paper proposed an integrated control method for floating offshore wind farms (FOWFs) with reconfigurable layouts, unifying turbine repositioning, wake steering, power derating, and dynamic wake mixing within a single framework. The controller operates in two modes: power maximization, where the objective is to increase total farm output, and power regulation, where the objective is to track a prescribed farm-level reference while mitigating wake interactions. The control problem is formulated as a nonlinear, nonconvex optimization and solved numerically using the FLORIS engineering wake model.



330



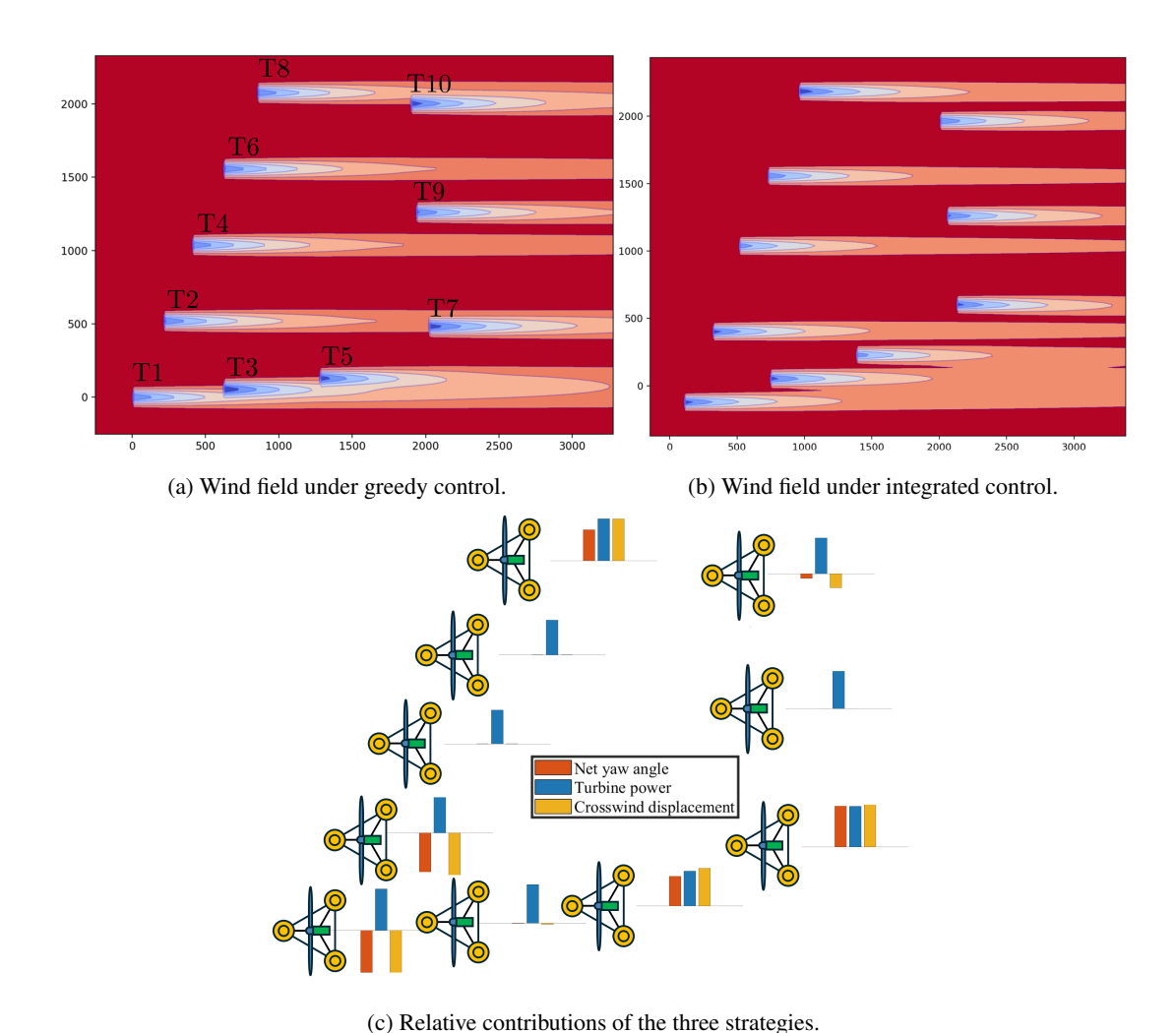


Figure 12. Control strategy contributions for regulation at  $P_{\text{ref}} = 45 \text{ MW}$  with inflow from the west.

Simulation studies demonstrated that the proposed controller successfully achieves these objectives. In maximization mode, it delivered up to 8.6% higher total power compared to baseline operation, while in regulation mode, it simultaneously tracked the prescribed farm-level reference and mitigated wake overlaps. The results further revealed how the integrated approach adapts to different wind conditions: in maximization mode, the controller prioritizes turbine repositioning when crosswind mobility is feasible, shifting adaptively to wake steering and dynamic wake mixing when mobility is restricted. In regulation mode, it achieves reference tracking through power derating, while coordinating turbine repositioning and wake steering to reduce wake interactions and downstream loading.

Overall, these findings demonstrate that coordinating multiple control strategies, rather than applying them in isolation, can significantly improve energy capture, reduce fatigue loading, and enhance operational flexibility in FOWFs. This work





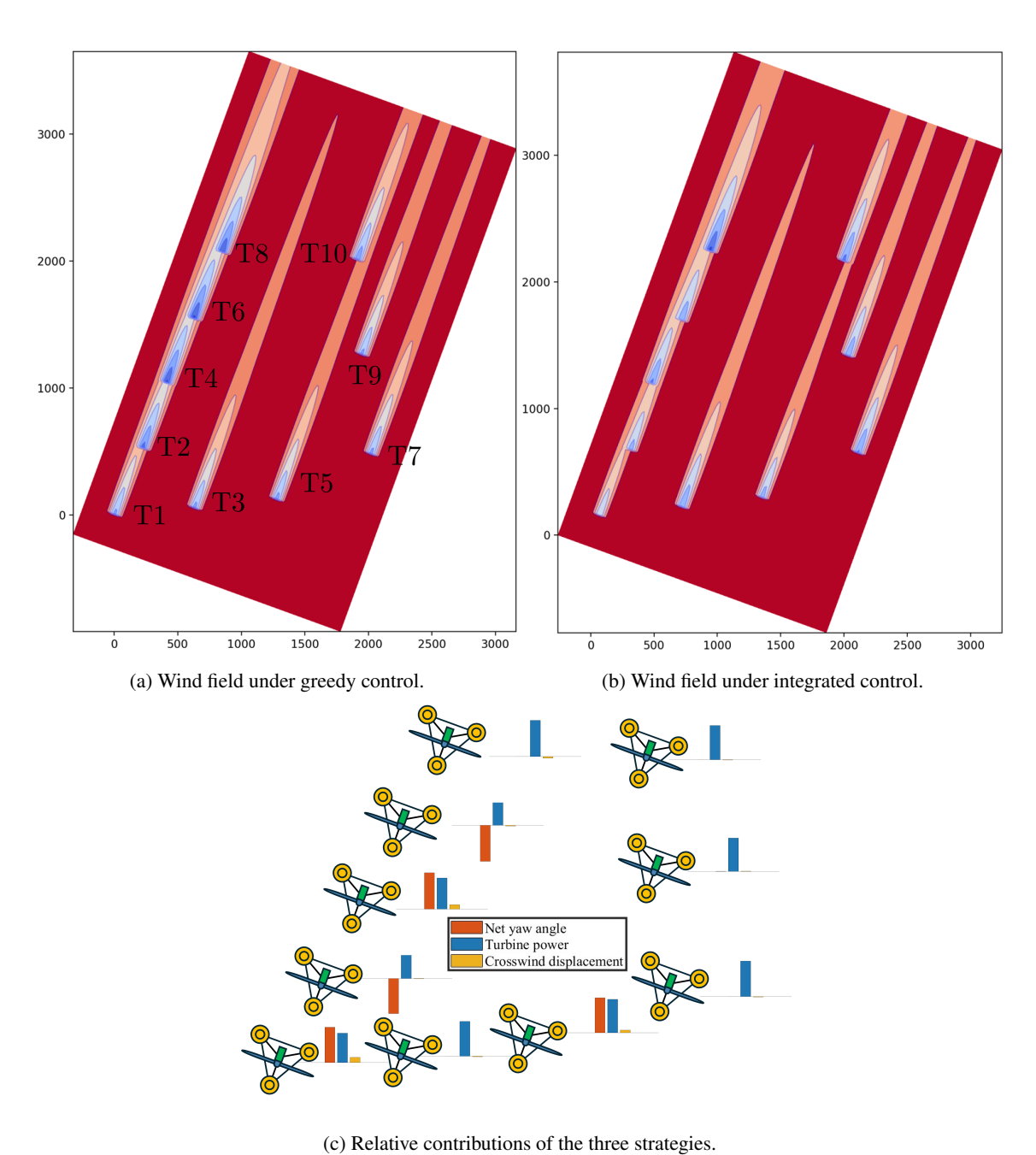


Figure 13. Control strategy contributions for regulation at  $P_{\rm ref}=45~{\rm MW}$  with inflow from the southwest.

Preprint. Discussion started: 19 November 2025

© Author(s) 2025. CC BY 4.0 License.



345



highlights the potential of integrated control frameworks to overcome the limitations of standalone methods and to support the broader deployment of floating offshore wind energy. Future work can extend the present framework toward control codesign: rather than assuming an FOWF is already installed, mooring system configurations could be optimized to ensure that at least a subset of turbines retains mobility under any wind condition, thereby further improving overall farm performance. Such

advancements will enhance the operational efficiency and economic viability of next-generation offshore wind energy systems.

340 *Code and data availability.* The code used in this study will be provided to reviewers through a private link. For other researchers, the code is available from the corresponding author upon reasonable request during the review process and will be made publicly available in a permanent repository upon publication.

Author contributions. YN contributed to the conceptualization, methodology, software, formal analysis, investigation, visualization, and writing (original draft preparation). RN contributed to the conceptualization, validation, writing (review and editing), supervision, project administration, and funding acquisition.

Competing interests. The authors declare that they have no conflict of interest.

Acknowledgements. The authors would like to thank Zekai Chen, Casey Heiskell, and Yuting Wu for their helpful discussions and constructive feedback during the course of this research.





#### References

360

- Andersson, L. E., Anaya-Lara, O., Tande, J. O., Merz, K. O., and Imsland, L.: Wind farm control Part I: A review on control system concepts and structures, IET Renewable Power Generation, 15, 2085–2108, 2021.
  - Barthelmie, R. J., Hansen, K., Frandsen, S. T., Rathmann, O., Schepers, J. G., Schlez, W., Phillips, J., Rados, K., Zervos, A., Politis, E. S., and Chaviaropoulos, P. K.: Modelling and measuring flow and wind turbine wakes in large wind farms offshore, Wind Energy, 12, 431–444, 2009.
- Boersma, S., Doekemeijer, B. M., Gebraad, P. M. O., Fleming, P. A., Annoni, J., Scholbrock, A. K., Frederik, J. A., and van Wingerden, J.-W.: A tutorial on control-oriented modeling and control of wind farms, in: 2017 American Control Conference, pp. 1–18, Seattle, WA, USA, https://doi.org/10.23919/ACC.2017.7962923, 2017.
  - Burton, T., Jenkins, N., Sharpe, D., and Bossanyi, E.: Wind Energy Handbook, Wiley, Hoboken, NJ, USA, 2nd edn., 2011.
  - Deb, K., Pratap, A., Agarwal, S., and Meyarivan, T.: A fast and elitist multiobjective genetic algorithm: NSGA-II, IEEE Transactions on Evolutionary Computation, 6, 182–197, 2002.
    - Doekemeijer, B. M., van Wingerden, J.-W., and Fleming, P. A.: A tutorial on the synthesis and validation of a closed-loop wind farm controller using a steady-state surrogate model, in: 2019 American Control Conference, pp. 2825–2836, Philadelphia, PA, USA, 2019.
    - Dong, H., Xie, J., and Zhao, X.: Wind farm control technologies: From classical control to reinforcement learning, Progress in Energy, 4, Art. no. 032006, 2022.
- Fleming, P., Gebraad, P. M. O., Lee, S., van Wingerden, J.-W., Johnson, K., Churchfield, M., Michalakes, J., Spalart, P., and Moriarty, P.: Simulation comparison of wake mitigation control strategies for a two-turbine case, Wind Energy, 18, 2135–2143, 2015.
  - Froese, G., Ku, S. Y., Kheirabadi, A. C., and Nagamune, R.: Optimal layout design of floating offshore wind farms, Renewable Energy, 190, 94–102, 2022.
- Gao, Y., Padmanabhan, A., Chen, O., Kheirabadi, A. C., and Nagamune, R.: A Baseline Repositioning Controller for a Floating Offshore
  Wind Farm, in: 2022 American Control Conference, pp. 4224–4229, Atlanta, GA, USA, 2022.
  - Goit, J. P. and Meyers, J.: Optimal control of energy extraction in wind-farm boundary layers, Journal of Fluid Mechanics, 768, 5–50, 2015. Han, C., Homer, J. R., and Nagamune, R.: Movable range and position control of an offshore wind turbine with a semi-submersible floating platform, in: 2017 American Control Conference, pp. 1389–1394, Seattle, WA, USA, 2017.
- Jard, T. and Snaiki, R.: Real-Time Repositioning of Floating Wind Turbines Using Model Predictive Control for Position and Power Regulation, Wind, 3, 131–150, 2023.
  - Johnson, K. E. and Thomas, N.: Wind farm control: Addressing the aerodynamic interaction among wind turbines, in: 2009 American Control Conference, pp. 2104–2109, St. Louis, MO, USA, 2009.
  - Jonkman, J., Butterfield, S., Musial, W., and Scott, G.: Definition of a 5-MW Reference Wind Turbine for Offshore System Development, Tech. Rep. NREL/TP-500-38060, National Renewable Energy Lab., Golden, CO, USA, 2009.
- Jonkman, J. M.: Dynamics of offshore floating wind turbines—model development and verification, Wind Energy, 12, 459–492, 2009.
  - Kheirabadi, A. C. and Nagamune, R.: A quantitative review of wind farm control with the objective of wind farm power maximization, Journal of Wind Engineering and Industrial Aerodynamics, 192, 45–73, 2019.
  - Kheirabadi, A. C. and Nagamune, R.: Real-time relocation of floating offshore wind turbine platforms for wind farm efficiency maximization: An assessment of feasibility and steady-state potential, Ocean Engineering, 208, Art. no. 107445, 2020.

https://doi.org/10.5194/wes-2025-240 Preprint. Discussion started: 19 November 2025

© Author(s) 2025. CC BY 4.0 License.



390



- 385 Kheirabadi, A. C. and Nagamune, R.: A low-fidelity dynamic wind farm model for simulating time-varying wind conditions and floating platform motion, Ocean Engineering, 234, Art. no. 109313, 2021a.
  - Kheirabadi, A. C. and Nagamune, R.: Real-time Relocation of Floating Offshore Wind Turbines for Power Maximization Using Distributed Economic Model Predictive Control, in: 2021 American Control Conference, pp. 3077–3081, New Orleans, LA, USA, 2021b.
  - Kilinc, U.: Dynamic wind farm layout optimization: To find the optimal spots for movable floating offshore wind turbines through dynamic repositioning, Master's thesis, Delft University of Technology, Delft, The Netherlands, 2022.
  - Mahfouz, M. Y. and Cheng, P.-W.: A passively self-adjusting floating wind farm layout to increase the annual energy production, Wind Energy, 26, 251–265, 2023.
  - Musial, W., Spitsen, P., Duffy, P., Beiter, P., Marquis, M., Hammond, R., and Shields, M.: Offshore Wind Market Report: 2022 Edition, Tech. Rep. DOE/GO-102022-5765, U.S. Department of Energy Office of Energy Efficiency & Renewable Energy, Washington, DC, USA, 2022.
- National Renewable Energy Laboratory: "FLORIS version 4.4.2." GitHub, https://github.com/NREL/floris, accessed: Aug. 22, 2025.
  - Niu, Y., Lathi, P. P., and Nagamune, R.: Floating Offshore Wind Farm Control via Turbine Repositioning with Aerodynamic Force, in: 2023 American Control Conference, pp. 2542–2547, San Diego, CA, USA, 2023.
  - Niu, Y., Dwivedi, A., Sathiaraj, J., Lathi, P. P., and Nagamune, R.: Floating Offshore Wind Farm Control via Turbine Repositioning: Unlocking the Potential Unique to Floating Offshore Wind, IEEE Control Systems, 44, 106–129, 2024.
- 400 Robertson, A., Jonkman, J., Masciola, M., Song, H., Goupee, A., Coulling, A., and Luan, C.: Definition of the Semisubmersible Floating System for Phase II of OC4, Tech. Rep. NREL/TP-5000-60601, National Renewable Energy Lab., Golden, CO, USA, 2014.
  - Steinbuch, M., de Boer, W. W., Bosgra, O. H., Peters, S. A. W. M., and Ploeg, J.: Optimal control of wind power plants, Journal of Wind Engineering and Industrial Aerodynamics, 27, 237–246, 1988.
- van den Berg, D., D. Tavernier, D., Marten, D., Saverin, J., and van Wingerden, J.-W.: Wake Mixing Control For Floating Wind Farms:

  Analysis of the Implementation of the Helix Wake Mixing Strategy on the IEA 15-MW Floating Wind Turbine, IEEE Control Systems,

  44, 81–105, 2024.